2010 IEEE International Conference on Robotics and Automation
Anchorage Convention District
May 3-8, 2010, Anchorage, Alaska, USA

Ankle and Hip Balance Control Strategies with Transitions

Yoshikazu Kanamiya, Shun Ota and Daisuke Sato

Abstract— **A method for implementing the ankle and hip balance control strategies, well known from studies on human balance control, is suggested. The moment of the acting disturbance force is evaluated continuously in real time via the difference between the ZMP and the ground projection of the center of mass. Compliant response to the continuous disturbance is ensured by attaching a virtual spring-damper in an appropriate way for each strategy. Further on, whenever the limit of the ankle strategy is reached, a smooth transition toward the hip strategy is initialized and compliance is ensured in a continuous way and in agreement with the disturbance. After the disturbance is removed, the humanoid switches first back to the ankle strategy, and then returns to the initial equilibrium (erect) posture. Experimental data taken with a small humanoid robot (HOAP-2) are presented to validate the method. See also the accompanying video clip.**

I. Introduction

The balance controller plays a central role within the overall control architecture of a humanoid robot. Similar to balance control in humans, the control objectives of the balance controller can be conditionally divided into two large groups [1]:

- balance control during proactive (preplanned) activities;
- balance control for reactive motion patterns, in response to unexpected disturbances from the environment.

Past research has mainly addressed the first type of control objective, e.g. balance control during steady gait [2], [3], or while lifting [4], pushing [5], or hitting [6] objects. Works, that addressed the second type of control objective, on the other hand, tackled such tasks as: keeping balance on unstable ground [7], keeping upright posture on a changing slope [8], walk on uneven terrain [9], maintaining balance when an obstacle appears suddenly in front of the robot [10]–[12], and balance recovery after the robot has been subjected to an unexpected external disturbance.

In this work, we focus on reaction pattern generation and control in the latter case, assuming that the robot will be exposed to unexpected disturbances. Research in this area has been mostly based on experimental data from studies on human balance control. Researchers have paid a lot of attention to balance recovery strategies in humans, in response to disturbance forces generated by horizontal perturbations in the support surface while standing upright. It was clarified that while standing on a normal surface, postural control is ensured via a reaction pattern called "ankle strategy," which restores equilibrium by motions in the ankle joints mainly. On the other hand, with a support surface shortened in relation to foot length, a different reaction pattern, called "hip strategy," was observed. This pattern produces a horizontal shear force against the support surface, with little or without any motion in the ankles, but with a predominant motion in the hips [1], [13]–[16]. In addition to these two strategies, a third strategy was identified — the "stepping" or "stumbling" strategy [15]. This strategy is invoked when certain boundary values (in position and/or velocity) during the hip strategy are exceeded. The three strategies are outlined in Fig. 1.

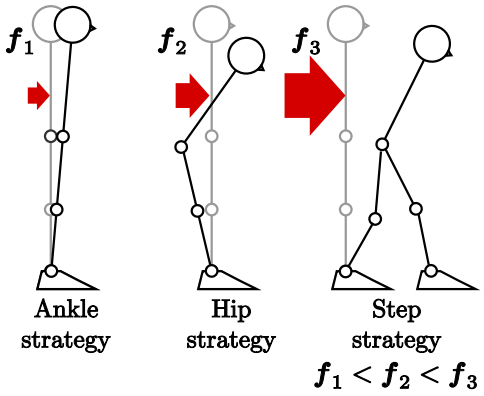

Fig. 1. Ankle, hip and step strategies.

Further on, a hypothesis exists that human postural control relies upon synthesis of complex motor actions by combining a limited number of simple response patterns, as some of the above mentioned [14]. It was pointed out [13] that from 63 possible combinations of leg muscle contractions, only six may be used in practice: four stemming from forward and backward ankle and hip strategies and two additional synergies from upward and downward motions, due to a "suspensory" strategy, generating reaction patterns in the vertical direction. In [1], it is mentioned that the ankle strategy includes also knee torque, and that the hip strategy adds hip torque to the ankle and knee torque. The role of the knee motion has been examined also elsewhere [13], [17]. Some authors use the name "combined strategy" for such reaction patterns [16].

In the field of humanoid robots, suggestion have been made about possible ways to adopt the ankle and hip strategies, so far [7], [18]–[20]. We have succeeded [21] in implementing the ankle and hip strategies as balance recovery patterns in response to *impact disturbances* on the back or on the chest of a small humanoid robot HOAP-2 [22]. In our case, the hip strategy was actually implemented as a

The authors are with the Department of Mechanical Systems Engineering, Tokyo City University, Tamazutsumi 1-28-1, Setagaya-ku, Tokyo 158-8557, Japan. Corresponding author: Y. Kanamiya (D. N. Nenchev) nenchev@tcu.ac.jp

The support by Grant-in-Aid for Scientific Research Kiban (B) 20300072 of JSPS is acknowledged.

combined strategy, involving an inverted double-pendulum model. We applied thereby the Reaction Null Space method, developed originally for base disturbance control of free-flying [23] or flexible-base mounted space robots [24]. We also have shown that the same method is useful for other types of disturbances, such as sudden motions in the support surface, i.e. slipping [25] and rotations [26].

The aim of the present work is twofold. Our first goal is to implement the ankle and hip strategies to respond to *continuous disturbances*. The second goal is to tackle the problem of smooth transitions between the two strategies, thus opening the way for generating more sophisticated response patterns.

II. Background and Notation

A. General form of the equation of motion

The equation of motion of an unconstrained underactuated system having a tree-like topological structure with n rotational joints, e.g. a humanoid robot in midair, is:

$$\begin{bmatrix} \boldsymbol{H}_b & \boldsymbol{H}_{bl} \\ \boldsymbol{H}_{bl}^T & \boldsymbol{H}_l \end{bmatrix} \begin{bmatrix} \dot{\boldsymbol{\nu}}_b \\ \ddot{\boldsymbol{\theta}} \end{bmatrix} + \begin{bmatrix} \boldsymbol{c}_b \\ \boldsymbol{c}_l \end{bmatrix} + \begin{bmatrix} \boldsymbol{g}_b \\ \boldsymbol{g}_l \end{bmatrix} = \begin{bmatrix} \boldsymbol{0} \\ \boldsymbol{\tau} \end{bmatrix}, \quad (1)$$

where

$\boldsymbol{H}_l$	$\in$	$\Re^{n\times n}$	:link inertia matrix
$\boldsymbol{H}_b$	$\in$	$\Re^{6\times 6}$	:inertia matrix of the base
$\boldsymbol{H}_{bl}$	$\in$	$\Re^{6\times n}$	:inertia coupling matrix
$\boldsymbol{c}_l$	$\in$	$\Re^n$	:link Coriolis and centrifugal forces
$\boldsymbol{c}_b$	$\in$	$\Re^6$	:base Coriolis and centrifugal forces
$\boldsymbol{g}_l$	$\in$	$\Re^n$	:link gravity force vector
$\boldsymbol{g}_b$	$\in$	$\Re^6$	:base gravity force vector
$\boldsymbol{\tau}$	$\in$	$\Re^n$	:joint torque vector
$\boldsymbol{\theta}$	$\in$	$\Re^n$	:joint coordinate vector
$\boldsymbol{\nu}_b$	$\in$	$\Re^6$	:base twist (spatial velocity)

In the above notation, "base" denotes a suitably chosen reference link. Note also that no external forces are present.

Let us assume now that the robot stands on the ground, balancing on one of its legs. Balance is controlled via the interaction wrench between the foot and the ground[1]. Hence, we select the foot in contact with the ground as the base. The equation of motion is rewritten then as:

$$\begin{bmatrix} \boldsymbol{H}_f & \boldsymbol{H}_{fl} \\ \boldsymbol{H}_{fl}^T & \boldsymbol{H}_l \end{bmatrix} \begin{bmatrix} \dot{\boldsymbol{\nu}}_f \\ \ddot{\boldsymbol{\theta}} \end{bmatrix} + \begin{bmatrix} \boldsymbol{c}_f \\ \boldsymbol{c}_l \end{bmatrix} + \begin{bmatrix} \boldsymbol{g}_f \\ \boldsymbol{g}_l \end{bmatrix} = \begin{bmatrix} \boldsymbol{0} \\ \boldsymbol{\tau} \end{bmatrix} + \begin{bmatrix} \boldsymbol{J}_{gf}^T \\ \boldsymbol{J}_{gl}^T \end{bmatrix} \boldsymbol{w}_g + \begin{bmatrix} \boldsymbol{J}_{ef}^T \\ \boldsymbol{J}_{el}^T \end{bmatrix} \boldsymbol{w}_e. \quad (2)$$

Here, the subscript "b" (base) has been changed to "f" (foot). Newly introduced terms on the r.h.s. are the constraint force and external force terms including the ground reaction wrench $\boldsymbol{w}_g$ and the external force wrench $\boldsymbol{w}_e$, respectively. The $\boldsymbol{J}_{\{\circ\}}$-terms denote proper transforms.

[1]No slip is assumed henceforth.

B. The Reaction Null Space of a humanoid

A humanoid robot can be described as an underactuated mechanical system with redundant DOFs. Balance control is ensured through appropriate link motion and the respective interaction wrenches between the links in contact with the environment. A measure for balance stability can be deduced from the Zero-Moment-Point (ZMP) [27]. Although the ZMP has been widely used as a means to control balance while standing or walking so far, it should be noted that ZMP-based stability measures do not account for the full state of the feet. Furthermore, the ZMP can be deduced only for ground contacts on flat surfaces.

Note, on the other hand, that there are many situations in practice whereby contact conditions cannot be simplified as in the case with the ZMP. In such situations, the full state of the links in contact must be accounted for. To deal with this problem, we transferred the concept of *Reaction Null Space* (RNS) from the field of space robotics [23], [24] to the field of humanoid robots [21]. Through the RNS, it is easy to obtain all link motions that keep the contact states unchanged. Further details follow below.

Consider first the *dynamic wrench* acting at the foot:

$$\boldsymbol{w}_d = \frac{d}{dt} \begin{bmatrix} m_t \dot{\boldsymbol{r}}_{cm} \\ \boldsymbol{r}_{cm} \times m_t \dot{\boldsymbol{r}}_{cm} + \sum_{j=0}^{n} (\boldsymbol{I}_j \boldsymbol{\omega}_j + \boldsymbol{r}_j \times m_j \dot{\boldsymbol{r}}_j) \end{bmatrix}, \quad (3)$$

where $\boldsymbol{r}_{cm}$ is the position of the total center of mass, $\boldsymbol{I}_j$, $\boldsymbol{\omega}_j$, m_j, $\boldsymbol{r}_j$ stand for the inertia matrix, angular velocity, mass and center-of-mass position for link j, respectively, and m_t is the total mass ($= \sum m_j$).

The dynamic wrench can be represented as a function of the generalized coordinates ($\boldsymbol{\xi}_f$, $\boldsymbol{\theta}$) and their time derivatives:

$$\boldsymbol{w}_d = \boldsymbol{H}_f \dot{\boldsymbol{\nu}}_f + \boldsymbol{w}_{fl}(\boldsymbol{\theta}, \dot{\boldsymbol{\theta}}, \ddot{\boldsymbol{\theta}}, \boldsymbol{\xi}_f, \boldsymbol{\nu}_f). \quad (4)$$

Here $\boldsymbol{\xi}_f$ denotes the spatial displacement of the foot. Note that we have separated the inertial wrench $\boldsymbol{H}_f \dot{\boldsymbol{\nu}}_f$ from the *imposed wrench* $\boldsymbol{w}_{fl}$. The latter is imposed on the foot through the motion of all other links; it is due to the inertial and nonlinear couplings between the foot and the rest of the links. From the upper part of (2), we can write:

$$\boldsymbol{w}_{fl}(\boldsymbol{\theta}, \dot{\boldsymbol{\theta}}, \ddot{\boldsymbol{\theta}}, \boldsymbol{\xi}_f, \boldsymbol{\nu}_f) = \boldsymbol{H}_{fl} \ddot{\boldsymbol{\theta}} + \boldsymbol{c}_f. \quad (5)$$

The *dynamic equilibrium of the foot* can then be expressed as:

$$\begin{aligned} \boldsymbol{w}_d + \boldsymbol{g}_f - \boldsymbol{J}_{gf}^T \boldsymbol{w}_g - \boldsymbol{J}_{ef}^T \boldsymbol{w}_e = \\ \boldsymbol{H}_f \dot{\boldsymbol{\nu}}_f + \boldsymbol{w}_{fl} + \boldsymbol{g}_f - \boldsymbol{J}_{gf}^T \boldsymbol{w}_g - \boldsymbol{J}_{ef}^T \boldsymbol{w}_e = \boldsymbol{0}. \end{aligned} \quad (6)$$

Assume now that the robot is initially motionless, in *static equilibrium* (the foot is at rest on the ground and the links are not moving). Hence, $\boldsymbol{\nu}_f = \boldsymbol{w}_{fl} = \boldsymbol{0}$, $\boldsymbol{g}_f = \boldsymbol{J}_{cf}^T \boldsymbol{w}_c + \boldsymbol{J}_{gf}^T \boldsymbol{w}_g$. Rewrite (5) as:

$$\boldsymbol{H}_{fl} \ddot{\boldsymbol{\theta}} + \dot{\boldsymbol{H}}_{fl} \dot{\boldsymbol{\theta}} = \boldsymbol{0}, \quad (7)$$

where $\boldsymbol{c}_f$ is approximated by the second term on the l.h.s. Since we have a redundant system at hand, the number of

joints is larger than the DOF of the foot ($n > 6$). Therefore, the general solution for the acceleration can be obtained from the above equation as:

$$\{\ddot{\boldsymbol{\theta}}_{RL}\} = -\boldsymbol{H}_{fl}^{\#}\dot{\boldsymbol{H}}_{fl}\dot{\boldsymbol{\theta}} + \{\mathcal{N}_{fl}\} \tag{8}$$

where $(\circ)^{\#}$ denotes a generalized inverse and $\{\mathcal{N}_{fl}\}$ stands for the kernel of the inertia coupling matrix $\boldsymbol{H}_{fl}$. The kernel can be determined e.g. as the set of vectors $\{(\boldsymbol{U} - \boldsymbol{H}_{fl}^{\#}\boldsymbol{H}_{fl})\boldsymbol{\zeta}\}$, $\boldsymbol{U}$ denoting the unit matrix and $\boldsymbol{\zeta}$ standing for an arbitrary n-vector. The kernel $\{\mathcal{N}_{fl}\}$ is referred to as the *Reaction Null Space* (RNS) of a humanoid robot (see also [21]).

The last equation shows that there is a set of link accelerations that would keep the imposed wrench on the foot zero throughout the motion ($\boldsymbol{w}_{fl}(t) = \boldsymbol{0}$, for any t). Hence, the *static equilibrium of the foot* will not be disturbed and the balance will be maintained despite the link motion. Any acceleration from the set $\{\ddot{\boldsymbol{\theta}}_{RL}\}$ can be therefore described as a *reactionless joint acceleration*.

Two remarks are due. First, from the definition of the dynamic wrench (3), it should be apparent that the total CoM will remain motionless[2] under reactionless joint accelerations. Second, in practice, not all of the components of the imposed wrench will need to be zeroed. The vertical downward force component, for example, may have nonzero values without disturbing the balance. The force components in the plane normal to the vertical may also have limited nonzero values, that will depend upon the friction coefficients. In these cases, a straightforward modification of the above equations can be done, as shown in [24] under the name "selective Reaction Null Space."

III. Responses to Continuous Disturbances under the Ankle and Hip Strategies

In our previous work [21], [25], we have introduced a way of implementing the ankle and hip strategies for generating response and balance recovery patterns with a small humanoid robot HOAP-2 [22], subjected to impacts on the back or on the chest while standing upright. The ankle and hip strategies are phenomena occuring in the sagittal plane. Therefore, simple planar models have been used to develop the response patterns for each of the strategies (see Fig. 2).

The ankle strategy was modeled with the help of a simple inverted pendulum (Fig. 2 (a)). A virtual spring–damper was attached to the ankle joint to ensure compliant response to the impact force. The initial response rate in that joint was calculated via impact force estimation from the built-in acceleration sensor.

The hip strategy, on the other hand, was modeled with the help of a double–inverted pendulum (Fig. 2 (b)). A virtual spring–damper was attached to the hip joint, thus ensuring compliant response to the impact force with predominant motion in the hip. In addition, the CoM ground projection

[2]With static initial conditions.

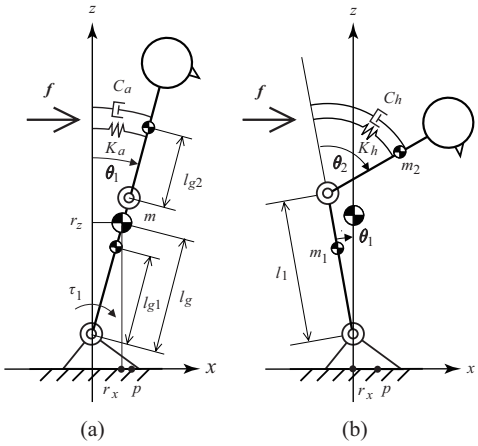

Fig. 2. Models for ankle (a) and hip (b) strategies.

was kept constant by applying the RNS method. Thus, a small compensatory motion in the ankle joint was generated.

In what follows, we will describe an extension of the method, such that the robot will be equipped with the ability to respond to a continuous external force, in addition to the impacts.

A. ZMP based ankle strategy

In the absence of external forces, the equation of motion for the model shown in Fig. 2 (a) can be written as:

$$(I + ml_g^2)\ddot{\theta}_1 - mgr_x = \tau_1 - C_a\dot{\theta}_1 - K_a\theta_1, \tag{9}$$

where $m = m_1 + m_2$ is the total mass, l_g is the distance from the ankle to the CoM, $r_x = l_g \sin\theta_1$ is the CoM ground projection, g is the gravity acceleration, I is the moment of inertia, and the other parameters are obvious from the model.

Further on, denote by p the position of the ZMP. Then, the moment equilibrium on the foot can be expressed as:

$$mg(p - r_x) = m\ddot{r}_x r_z + m\ddot{r}_z(p - r_x), \tag{10}$$

where $r_z = l_g \cos\theta_1$ is the vertical projection of the CoM. A torque in the ankle joint changes the foot moment, hence we can write: $mg(p - r_x) = \tau_1$. This is true also for an external force applied at the CoM: $mg(p - r_x) = fr_z$. Incorporating these relations under simplifying assumption into the equation of motion (9), we can derive the ankle joint acceleration as:

$$\ddot{\theta}_1^{ref} = \frac{1}{I + ml_g^2}\left(mg\,(p - r_x) - C_a\dot{\theta}_1 - K_a\theta_1\right). \tag{11}$$

This is integrated twice to obtain the reference joint angle to be used as real-time control input for the robot balance controller.

B. ZMP based hip strategy

The extension of the hip strategy implementation, as described in our previous work [21], [25], is as straightforward as that of the ankle strategy. We apply again the RNS method. Considering (7), we note first that, for the double inverted-pendulum model under consideration, the coupling inertia

$\boldsymbol{H}_{fl} \in \Re^{1\times 2}$ and the joint coordinate vector contains the two joint angles (ankle and hip). Further on, integrate (7) to obtain the constant coupling momentum:

$$\boldsymbol{H}_{fl}\dot{\boldsymbol{\theta}} = \boldsymbol{\mathcal{L}}. \tag{12}$$

Zero initial conditions are assumed: $\boldsymbol{\mathcal{L}} = \mathbf{0}$. Hence, we obtain the following set of *reactionless joint velocities*:

$$\{\dot{\boldsymbol{\theta}}_{RL}\} = \{b\boldsymbol{n}\}, \tag{13}$$

where b is an arbitrary scalar and $\boldsymbol{n} \in \Re^2$ is in the kernel of $\boldsymbol{H}_{fl}$. Referring to the model in Fig. 2 (b), we can write:

$$\boldsymbol{n} = \begin{bmatrix} -m_2 l_{g2} C_{12} \\ (m_1 l_{g1} + m_2 l_1)\, C_1 + m_2 l_{g2} C_{12} \end{bmatrix}, \tag{14}$$

where $C_1 = \cos\theta_1$ and $C_{12} = \cos(\theta_1 + \theta_2)$. Then, from (13) and (14) we obtain the following relation:

$$\dot{\theta_1}^{ref} = \frac{-m_2 l_{g2} C_{12}}{(m_1 l_{g1} + m_2 l_1) C_1 + m_2 l_{g2} C_{12}} \dot{\theta_2}^{ref}. \tag{15}$$

$\dot{\theta_2}^{ref}$ is the reference hip joint rate. It is calculated from the single inverted pendulum equation for the upper body link. Referring to (11), we can write:

$$\ddot{\theta_2}^{ref} = \frac{1}{I_2 + m_2 l_{g2}^2} \left(m_2 g\,(p - r_x) - C_h \dot{\theta}_2 - K_h \theta_2 \right), \tag{16}$$

where I_2 is the inertia moment of the upper body, and the rest of the parameters should be clear from Fig. 2.

IV. Transition between Ankle and Hip Strategies

Consider the displacement of the CoM during the two strategies. As seen from Fig. 2 (a), during the ankle strategy, the CoM is displaced in a way that its ground projection r_x remains within the base of support (BoS). On the other hand, during the hip strategy, the CoM is displaced only in the vertical direction, whereas its ground projection remains stationary (cf. Fig. 2 (b)).

The aim of the transition between the ankle and the hip strategy is to ensure that, in addition to hip motion initialization, the CoM ground projection will also move back swiftly to the position of the erected posture, after reaching the BoS boundary during the ankle strategy.

In order to ensure such movement of the CoM, we have to consider the CoM velocity:

$$\dot{\boldsymbol{r}} = \boldsymbol{J}_c \dot{\boldsymbol{\theta}}, \tag{17}$$

where $\boldsymbol{J}_c \in \Re^{2\times 2}$ denotes the CoM Jacobian matrix. This equation is projected onto the x axis:

$$\dot{r}_x = \boldsymbol{J}_{cx} \dot{\boldsymbol{\theta}}. \tag{18}$$

Note that matrix $\boldsymbol{J}_{cx} \in \Re^{1\times 2}$ is related to the coupling inertia matrix:

$$\boldsymbol{J}_{cx} = \frac{1}{m} \boldsymbol{H}_{fl}. \tag{19}$$

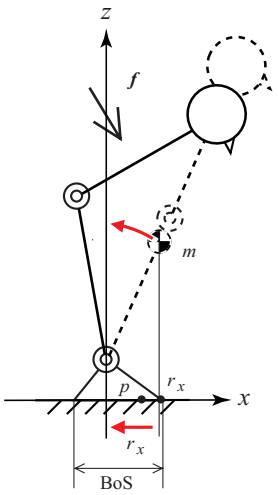

Fig. 3. Transition between ankle and hip strategies.

From the model, it is straightforward to obtain:

$$\boldsymbol{J}_{cx} = \begin{bmatrix} r_z & k_m l_{g2} C_{12} \end{bmatrix}, \tag{20}$$

where $k_m = m_2/m$. Hence, the solution to (18) can be written as:

$$\dot{\boldsymbol{\theta}} = \boldsymbol{J}_{cx}^{\#} \dot{r}_x + b\boldsymbol{n}. \tag{21}$$

Henceforth, we will use the pseudoinverse as a generalized inverse.

V. Transition Control

Consider first the ankle–hip transition phase. By making use of (14) and (20), (21) can be expanded in the following form:

$$\begin{bmatrix} \dot{\theta}_1 \\ \dot{\theta}_2 \end{bmatrix} = \frac{\dot{r}_x^{ref}}{r_z^2 + (k_m l_{g2} C_{12})^2} \begin{bmatrix} r_z \\ k_m l_{g2} C_{12} \end{bmatrix} + b \begin{bmatrix} -m_2 l_g C_{12} \\ (m_1 l_{g1} + m_2 l_1)\, C_1 + m_2 l_{g2} C_{12} \end{bmatrix}. \tag{22}$$

From this equation, we can derive the reference ankle joint rate as:

$$\dot{\theta}_1^{ref} = \frac{r_z}{r_z^2 + (k_m l_g C_{12})^2} \dot{r}_x^{ref} + k_w \frac{-m_2 l_g C_{12}}{(m_1 l_{g1} + m_2 l_1)\, C_1 + m_2 l_{g2} C_{12}} \dot{\theta}_2. \tag{23}$$

The first component on the r.h.s. is responsible for the rate of the CoM ground projection, while the second one ensures reactionless joint velocity (see also (15)). Note, however, that the two objectives are contradictive: the first component implies motion of the CoM, while the second one — a stationary CoM ground projection, when generating a reactionless joint velocity. To deal with this problem, we introduced a variable weight coefficient $0 \le k_w \le 1$.

The reference CoM rate is calculated via the simple P feedback control equation:

$$\dot{r}_x^{ref} = K_{pr} \left(r_x^d - r_x \right), \tag{24}$$

TABLE I

MOTION PHASES AND VARIABLES.

Phase	Strategy	θ_1	θ_2	Variable of transition
I	Ankle	(11)	-	-
II	A–H transition	(23)(24) r_x^d: $r_x^{lim} \xrightarrow{\text{spline}} r_x^{init}$	(16) k_w: $0 \xrightarrow{\text{spline}} 1$	p
III	Hip	(15)	(16)	-
IV	H–A transition	(11)	(25)	p, r_z
V (I')	Ankle	(11)	-	-

K_{pr} denoting a positive feedback gain. The desired r_x^d is calculated via a fifth-order spline function to ensure smooth transition between the values r_x^{lim} and $r_x^{init}(=0)$, where r_x^{lim} is the value of the CoM ground projection at the time instant when $p = p^{lim}$. p^{lim}, in turn, is a safety limit for the ZMP position, usually set close to the foot toe. The variable weight coefficient k_w is also calculated via a fifth-order spline.

To initialize the hip–ankle transition, the values of the ZMP (p) and the vertical CoM coordinate (r_z) are monitored. Note that the desired posture at the end of the transition equals the initial (erect) one ($\theta_2 = 0$). With proper values, the transition will be initialized when θ_2 is close to zero. Hence, a regulator type feedback controller can be employed:

$$\dot{\theta}_2 = -K_{p\theta}\theta_2, \tag{25}$$

$K_{p\theta}$ denoting a positive feedback gain.

At the end, we obtain four distinct phases of motion. These are summarized in Table I, where A–H stands for ankle–hip, and H–A for hip–ankle.

VI. EXPERIMENT

For the ankle strategy, the inverted pendulum model (11) is used. For the hip strategy, the inverted pendulum (16) is used for the hip joint, while (23) is employed for the ankle joint. The virtual spring-damper values were set empirically, as follows: $C_a = 10000$ Nm·s/rad, $K_a = 40000$ Nm/rad, $C_h = 1000$ Nm·s/rad, $K_h = 4000$ Nm/rad. The P feedback gain values were set as $K_{p\theta} = 15$ s^{-1} and $K_{pr} = 100$ s^{-1}.

The time span for the A–H transition was set to 1 s, within the spline functions for variables k_w and r_x^d. The ZMP safety limit was set as $p^{lim} = 45$ mm. The H–A transition was initialized when the following condition was met: $264.5 < r_z < 266.5$ mm and $p < 0$.

Five cycles were executed during a time interval of 60 s, by applying five arbitrary external disturbances to the back of a HOAP-2 robot. The joint angle time history is shown in Fig. 4. It is seen that the robot always responded in a stable way. To gain further insight, we zoom in just at the first cycle. The respective detailed experimental data, including joint angles, ZMP position, CoM ground projection and the difference $p - r_x$, denoting the moment of the disturbance, are shown in Fig. 5. Snapshots taken during the first cycle of the experiment are shown in Fig. 6.

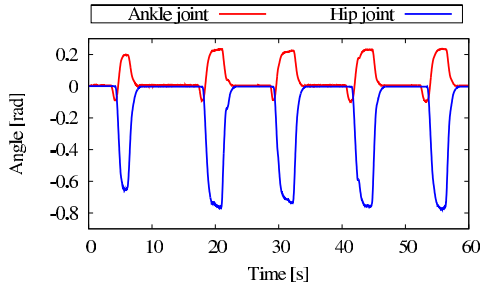

Fig. 4. Joint angle data from five cycles of applied disturbances.

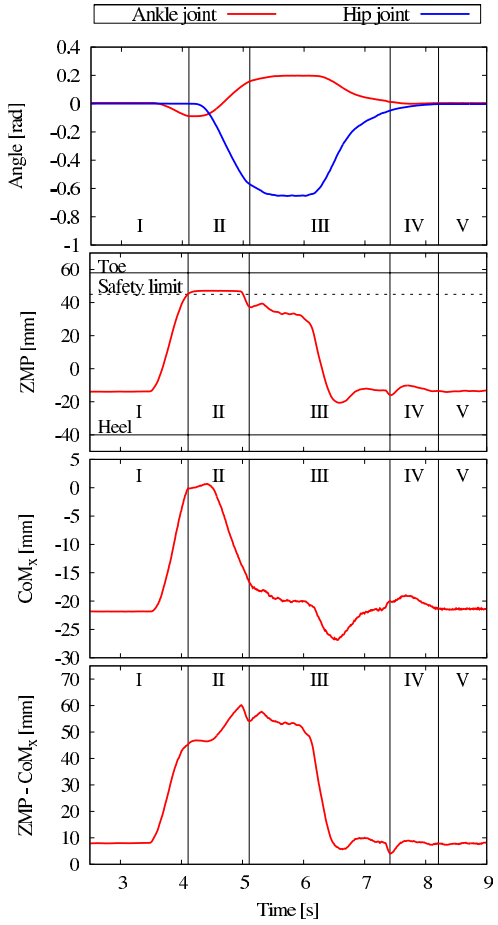

Fig. 5. Detailed data for the first motion cycle.

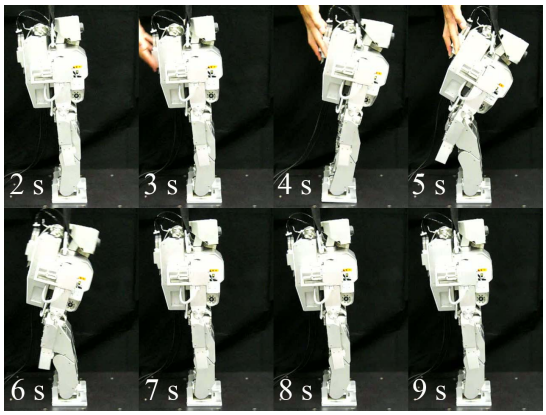

Fig. 6. Snapshots from the first cycle of the experiment.

From the data, it is seen that the robot is able to react to the disturbances as desired, switching smoothly between the two strategies. This can also be confirmed via the accompanying video clip.

VII. Conclusions

We described a method for implementing two balance control strategies, well known from studies on human balance control, to generate proper responses, when an unknown continuous external force is applied to a humanoid robot. The moment of the acting disturbance force is evaluated continuously in real time through the difference between the ZMP and the ground projection of the CoM. Compliant response to the continuous disturbance is ensured by attaching a virtual spring-damper in an appropriate way for each strategy.

Another contribution is the suggested method of transition control between the two strategies. Transition control is an important step toward generating more complex responses, based on simple response patterns, such as the two strategies under consideration.

The models used in this work are simple planar models. In a future work, we intend to implement the method in 3D in order to incorporate a third well known balance strategy — the stepping strategy— and to explore generation of more complex reaction and balance recovery patterns via suitable transitions between the strategies.

References

[1] F. B. Horak, S. M. Henry and A. Shumway-Cook, "Postural perturbations: new insights for treatment of balance disorders," *Physical Therapy*, vol. 77, no. 5, pp. 517–533, May 1997.

[2] S. Kajita *et al*., "Biped Walking Pattern Generation by using Preview Control of Zero–Moment Point," in *Proc. of the 2003 IEEE Int. Conf. on Robotics and Automation*, Taipei, Taiwan, 2003, pp. 1620–1626.

[3] T. Sugihara, Y. Nakamura and H. Inoue, "Realtime Humanoid Motion Generation through ZMP Manipulation based on Inverted Pendulum Control," in *Proc. of the 2002 IEEE Int. Conf. on Robotics and Automation*, Washington D.C., USA, 2002, pp. 1404–1409.

[4] K. Harada *et al*., "A Humanoid Robot Carrying a Heavy Object," in *Proc. of the 2005 IEEE Int. Conf. on Robotics and Automation*, Barcelona, Spain, 2005, pp. 1712–1717.

[5] K. Harada, S. Kajita, K. Kaneko and H. Hirukawa, "Pushing manipulation by humanoid considering two-kinds of ZMPs," in *Proc. of the 2003 IEEE Int. Conf. on Robotics and Automation*, Taipei, Taiwan, 2003, pp. 1627–1632.

[6] T. Matsumoto, A. Konno, L. Gou and M. Uchiyama, "A Humanoid Robot that Breaks Wooden Boards Applying Impulsive Force," in *Proc. of the 2006 IEEE/RSJ Int. Conf. on Intelligent Robots and Systems*, Beijing, China, 2006, pp. 5919–5924.

[7] M. Abdallah and A. Goswami, "A Biomechanically Motivated Two-Phase Strategy for Biped Upright Balance Control," in *Proc. of the 2005 IEEE Int. Conf. on Robotics and Automation*, Barcelona, Spain, 2005, pp. 1996–2001.

[8] J. S. Gutmann, M. Fukuchi and M. Fujita, "Stair Climbing for Humanoid Robots Using Stereo Vision" in *Proc. of the 2004 IEEE Int. Conf. on Intelligent Robots and Systems*, Sendai, Japan, 2004, pp. 1407–1413.

[9] S. Kajita *et al*., "Biped Walking Pattern Generator allowing Auxiliary ZMP Control," in *Proc. of the 2006 IEEE Int. Conf. on Intelligent Robots and Systems*, Beijing, China, 2006, pp. 2993–2999.

[10] M. Morisawa *et al*., "Motion Planning of Emergency Stop for Humanoid Robot by State Space Approach," in *Proc. of the 2006 IEEE Int. Conf. on Intelligent Robots and Systems*, Beijing, China, 2006, pp. 2986–2992.

[11] T. Tanaka *et al*., "Emergent stop for Humanoid Robots," in *Proc. of the 2006 IEEE Int. Conf. on Intelligent Robots and Systems*, Beijing, China, 2006, pp. 3970–3975.

[12] K. Kaneko *et al*., "Motion Suspension System for Humanoids in case of Emergency - Real-time Motion Generation and Judgment to suspend Humanoid -," in *Proc. of the 2006 IEEE Int. Conf. on Intelligent Robots and Systems*, Beijing, China, 2006, pp. 5496–5503.

[13] L. M. Nashner and G. McCollum, "The organisation of human postural movements: a formal basis and experimental hypothesis," *Behavioral and Brain Sciences*, vol. 8, pp. 135–172, 1985.

[14] F.B. Horak and L. M. Nashner, "Central programming of postural movements: adaptation to altered support surface configurations," *J. of Neurophysiology*, vol. 55, no. 6, pp. 1369–1381, June 1986.

[15] A. Shumway-Cook and F. B. Horak, "Vestibular Rehabilitation: An Exercise Approach to Managing Symptoms of Vestibular Dysfunction," *Seminars in Hearing*, vol. 10, no. 2, pp. 196–209, 1989.

[16] D. A. Winter, "Human balance and posture control during standing and walking," *Gait and Posture*, vol. 3 pp. 193–214, Dec. 1995.

[17] K. Iqbal and Y. Pai, "Predicted region of stability for balance recovery: motion at the knee joint can improve termination of forward movement," *J. of Biomechanics*, vol. 33, pp. 1619–1627, 2000.

[18] P. Gorce, "Dynamic Postural Control Method for Biped in Unknown Environment," *IEEE Tr. SMC, Part A: Systems and Humans*, vol. 29, no. 6, pp. 616–626, Nov. 1999.

[19] M. Guihard and P. Gorce, "Dynamic Control of Bipeds Using Ankle and Hip Strategies," in *Proc. of the 2002 IEEE/RSJ Int. Conf. on Intelligent Robots and Systems*, Lausanne, Switzerland, 2002, pp. 2587–2592.

[20] C. Azevedo, P. Poignet and B. Espiau, "Artificial Locomotion Control: From Human to Robots," *Robotics and Autonomous Systems*, vol. 47, no. 4, pp. 203–223, 2004.

[21] D. N. Nenchev and A. Nishio, "Ankle and Hip Strategies for Balance Recovery of a Biped Subjected to an Impact," *Robotica*, vol. 26, pp. 643–653, June 2008.

[22] *Miniature Humanoid Robot HOAP–2 Instruction Manual*, Fujitsu Automation Co., Ltd, Japan.

[23] D. N. Nenchev and K. Yoshida, "Impact Analysis and Post-Impact Motion Control Issues of a Free–Floating Space Robot Subject to a Force Impulse," *IEEE Trans. Robot. Autom.*, vol. 15, no. 3, pp. 548–557, June 1999.

[24] D. N. Nenchev, K. Yoshida, P. Vichitkulsawat and M. Uchiyama, "Reaction Null–Space Control of Flexible Structure Mounted Manipulator Systems," *IEEE Trans. on Robot. Autom.*, vol. 15, no. 6, pp. 1011–1023, Dec. 1999.

[25] A. Nishio, K. Takahashi and D. N. Nenchev, "Balance Control of a Humanoid Robot Based on the Reaction Null Space Method," *Proc. of the 2006 IEEE/RSJ Int. Conf. on Intelligent Robots and Systems*, Oct. 9 – 15, 2006, Beijing, China, pp. 1996–2001.

[26] K. Tamegaya, Y. Kanamiya, M. Nagao and D. Sato, "Inertia-Coupling Based Balance Control of a Humanoid Robot on Unstable Ground," in *Proc. of the 8th IEEE-RAS Int. Conf. on Humanoid Robots*, Daejeon, Korea, 2008, pp. 151–156.

[27] M. Vukobratovic and B. Borovac, "Zero Moment Point. Thirty Five Years of its Life," Int. J. Humanoid Robot, vol. 1, no. 1, pp. 157–173. 2004.